CONFIDENCE REGIONS FOR RTK GPS RECEIVERS

By Thomas G. Davis[1], Ph.D., P.E., P.L.S., M. ASCE

Abstract: Confidence regions based on typical manufacturer's accuracy specifications for geodetic-quality, real-time kinematic (RTK) global positioning system (GPS) receivers are developed and discussed.

INTRODUCTION

The considerable confusion surrounding GPS confidence regions is caused in part by ambiguous or incomplete manufacturer's accuracy specifications (Appendix I) and the evolution of horizontal accuracy standards from one (FGCC 1989) to two (FGDC 1998) dimensions. An accuracy statistic is not meaningful unless the number of dimensions to which it applies is specified together with the probability or level of confidence (USACE 2003). The root mean square error (rmse, rms, or mse) designation indicates a one-dimensional (1D) probability of 68.3%, two-dimensional (2D) probability of 63.2%, or three-dimensional (3D) probability of 60.8%. The standard error, standard deviation, or one-sigma level qualifier indicates a 68.3% probability in one dimension, 39.4% probability in two dimensions, and only 19.9% probability in three dimensions. Pertinent properties of the multivariate normal and chi-square distributions are presented in Appendices II, III, and IV.

None of the manufacturers of RTK GPS receivers surveyed here (Leica, NavCom, Sokkia, Thales, Topcon, Trimble) includes a dimension specification on their datasheets, and some datasheets include no qualifier whatsoever (Javad 2006; Thales 2006; Topcon 2004, 2005) but manufacturers' technical papers (Abousalem et al. 2001; Large et al. 2001) make it clear that the published accuracy values are 1D standard errors.

The 2D horizontal and 1D vertical accuracy standards presented here are endorsed by the Federal Geographic Data Committee (FGDC 1998) and incorporated by reference in Florida Administrative Code, Chapter 61G17-6.0051 (FAC 2005).

NUMERICAL EXAMPLE

Typical manufacturer's accuracy specifications (Table 2) are 10 mm + 1 ppm (part per million) horizontal and 20 mm + 1 ppm vertical at the one-dimensional, one-sigma standard error level. Considering a baseline length of 5 km, the 1D standard errors are

$$\sigma_x = 10 \text{ mm} + 5 \text{ km } (1 \text{ mm/km}) = 1.5 \text{ cm}, \quad (1a)$$
$$\sigma_y = 10 \text{ mm} + 5 \text{ km } (1 \text{ mm/km}) = 1.5 \text{ cm, and} \quad (1b)$$
$$\sigma_z = 20 \text{ mm} + 5 \text{ km } (1 \text{ mm/km}) = 2.5 \text{ cm}. \quad (1c)$$

where σ_x, σ_y, and σ_z are the semi-axes of the standard error ellipsoid (Fig. 5).

---

[1] Vice President of Surveying, Metzger & Willard, Inc., 8600 Hidden River Parkway, Suite 550, Tampa, FL 33637. E-mail: tdavis@metzgerwillard.com

1D Vertical Accuracy

Scaling the 1D standard vertical error (1c) to the 1D 95% confidence level (Fig. 3, Table 3)

$$\sigma_{Vertical} = 1.9600\ \sigma_z = 4.9 \text{ cm.} \tag{2}$$

Featherstone and Stewart (2001) report a 1D 95% vertical accuracy of 5.3 cm for 707 occupations of 61 points with baseline lengths up to 5 km.

2D Horizontal Accuracy

Scaling the 1D standard horizontal errors (1a, 1b) to the 2D 95% confidence level (Fig. 4, Table 3)

$$\sigma_{Horizontal} = 2.4477\ (\sigma_x + \sigma_y) / 2 = 3.7 \text{ cm.} \tag{3}$$

The 95% horizontal and vertical confidence regions for a point with true position (0,0,0) are depicted in Fig. 1. The horizontal confidence region is an infinitely long cylinder with radius 3.7 cm. The vertical confidence region is an infinite slab with upper and lower bounds at z = ± 4.9 cm.

Note well that the horizontal and vertical confidence regions are independent. The standard (FGDC 1998) does not require that a point meet the horizontal and vertical thresholds simultaneously. Thus, the point (-4,-4,0) cm (Fig. 1) satisfies the vertical standard, and the point (0,0,9) cm satisfies the horizontal standard. That is, the horizontal standard makes no simultaneous requirement of the z value, and the vertical standard makes no simultaneous requirements of the x and y values.

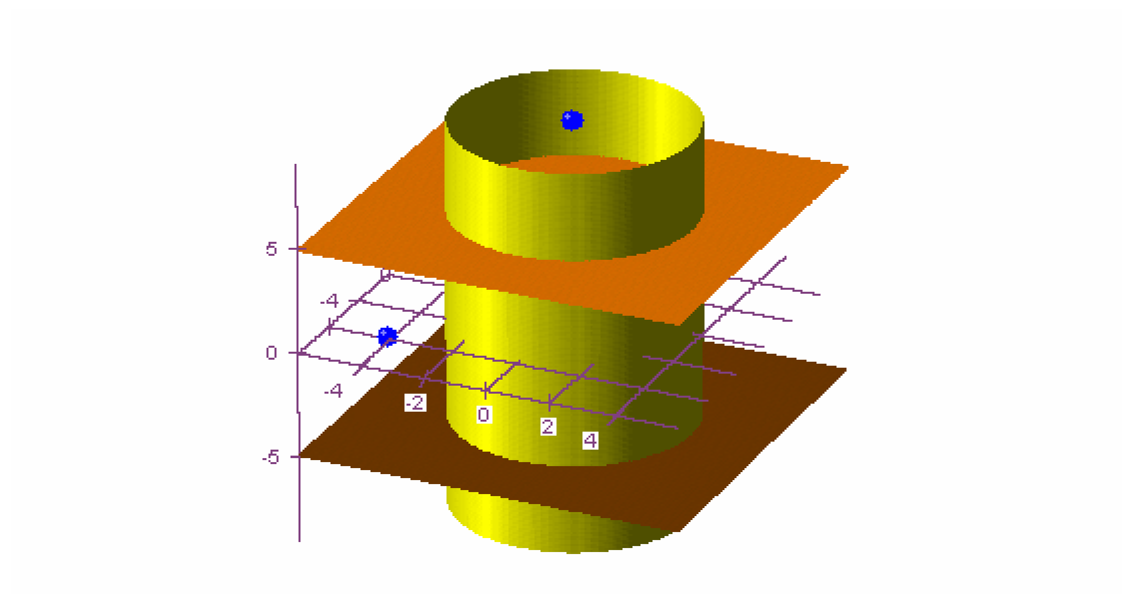

Figure 1. 2D Horizontal and 1D Vertical 95% Confidence Regions

3D Accuracy

If it is desired to simultaneously specify 95% thresholds for x, y, and z values, then the 1D standard errors (1) are scaled to the 3D 95% confidence level (Fig. 5, Table 3) by

$$\sigma_{3Dx} = 2.7955\ \sigma_x = 4.2 \text{ cm}, \tag{4a}$$
$$\sigma_{3Dy} = 2.7955\ \sigma_y = 4.2 \text{ cm, and} \tag{4b}$$
$$\sigma_{3Dz} = 2.7955\ \sigma_z = 7.0 \text{ cm} \tag{4c}$$

where σ_{3Dx}, σ_{3Dy}, and σ_{3Dz} are the semi-axes of the 95% confidence ellipsoid (Fig. 2a).

Another common measure of 3D accuracy is the 95% confidence sphere (Fig. 2b). Davis and Kleder (2006) rigorously compute a spherical radius (Appendix IV) which is approximated by

$$\sigma_{Spherical} = 0.9285 + 2.3816\ \sigma_{Avg} + 0.0591\ \sigma_{Avg}^2 = 5.5 \text{ cm} \tag{5}$$

where $\sigma_{Avg} = (\sigma_x + \sigma_y + \sigma_z) / 3 = 1.8333$ cm.

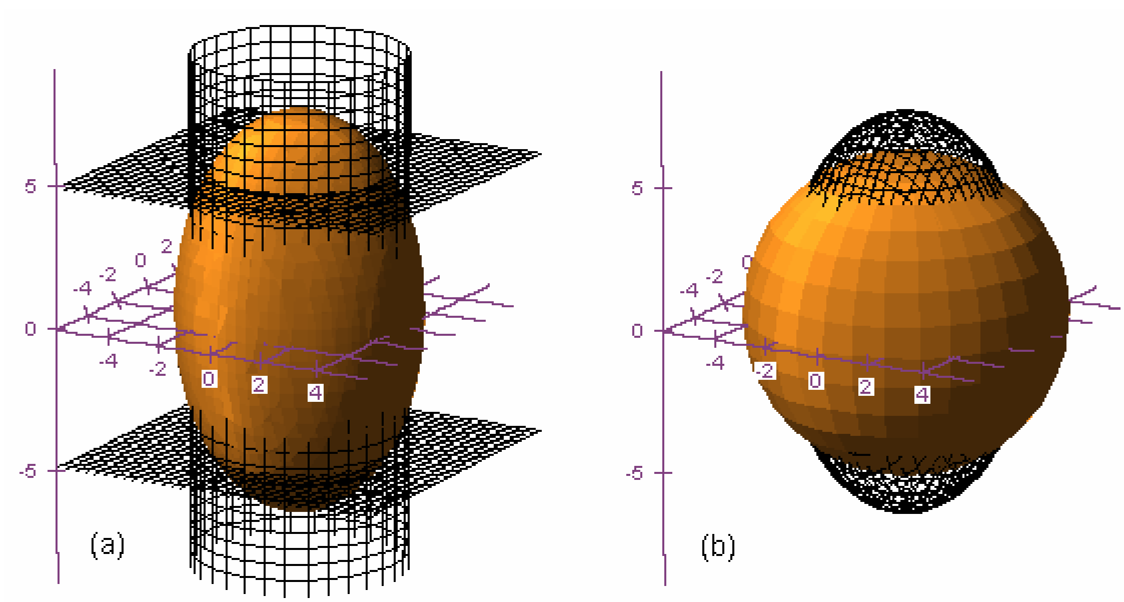

Figure 2. 3D 95% Confidence Regions: (a) Ellipsoid; (b) Sphere

CONCLUSIONS

The National Standard for Spatial Data Accuracy (FGDC 1998) establishes (2) and (3) as the vertical and horizontal accuracy, respectively, for a typical RTK GPS receiver with a baseline length of 5 km. It is expected that 95% of measured (x,y) values will lie within a planimetric circle centered at the true position with radius 3.7 cm. Similarly, it is expected that 95% of measured z values will lie within a vertical interval centered at the true position with semi-length 4.9 cm. These two facts do not, however, give rise to a 3D or overall accuracy. Instead, it is expected that 95% of measured (x,y,z) values will lie within an ellipsoid centered at the true position with semi-axes (4).

For a typical RTK GPS receiver with a baseline length of 5 km, points with horizontal deviations ranging up to 4.2 cm and points with vertical deviations ranging up to 7.0 cm are entirely normal at the 95% level and do not indicate unmodeled systematic errors or blunders. Table 1 shows typical accuracies with baseline lengths up to 20 km.

Table 1. 95% Horizontal, Vertical, and Spherical Accuracies

Baseline Length (km)	Accuracy (cm)				
	2D Horizontal	1D Vertical	3D Horizontal	3D Vertical	3D Spherical
0	2.4	3.9	2.8	5.6	4.2
1	2.7	4.1	3.1	5.9	4.5
2	2.9	4.3	3.4	6.2	4.7
3	3.2	4.5	3.6	6.4	5.0
4	3.4	4.7	3.9	6.7	5.2
5	3.7	4.9	4.2	7.0	5.5
6	3.9	5.1	4.5	7.3	5.8
7	4.2	5.3	4.8	7.5	6.0
8	4.4	5.5	5.0	7.8	6.3
9	4.7	5.7	5.3	8.1	6.5
10	4.9	5.9	5.6	8.4	6.8
11	5.1	6.1	5.9	8.7	7.1
12	5.4	6.3	6.2	8.9	7.3
13	5.6	6.5	6.4	9.2	7.6
14	5.9	6.7	6.7	9.5	7.9
15	6.1	6.9	7.0	9.8	8.2
16	6.4	7.1	7.3	10.1	8.4
17	6.6	7.3	7.5	10.3	8.7
18	6.9	7.4	7.8	10.6	9.0
19	7.1	7.6	8.1	10.9	9.2
20	7.3	7.8	8.4	11.2	9.5

All accuracy values assume single-base RTK operation with standard errors of 10 mm + 1 ppm horizontal and 20 mm + 1 ppm vertical. Factors including atmospheric conditions, satellite geometry, occupation times, multipath effects, obstructions, survey procedures, and base station data quality will affect performance (Appendix I).

APPENDIX I. MANUFACTURERS' SPECIFICATIONS

Table 2 summarizes manufacturers' accuracy specifications for geodetic-quality RTK GPS receivers.

Table 2. Manufacturers' Specifications

Manufacturer	Receiver	Accuracy		Accuracy Level
		Horizontal	Vertical	
Leica	GPS1200[1]	10 mm + 1 ppm	20 mm + 1 ppm	rms[10]
NavCom	RT-3010S[2]	10 mm + 1 ppm	20 mm + 1 ppm	rms
Sokkia	GSR2600[3]	10 mm + 1 ppm	20 mm + 1 ppm	1 sigma[10]
	GSR2700 IS[3]	10 mm + 1 ppm	20 mm + 1 ppm	1 sigma
	Radian IS[3]	10 mm + 1 ppm	20 mm + 1 ppm	1 sigma
Thales	Z-Max[4]	10 mm + 1 ppm	20 mm + 1 ppm	--[11]
	Z-Xtreme[5]	10 mm + 2 ppm[8]	20 mm + 2 ppm	rms
Topcon	HiPer Plus[6]	10 mm + 1 ppm[9]	15 mm + 1 ppm[9]	--
	HiPer XT[6]	10 mm + 1 ppm[9]	15 mm + 1 ppm[9]	--
Trimble	5700 GPS[7]	10 mm + 1 ppm	20 mm + 1 ppm	rms
	5800 GPS[7]	10 mm + 1 ppm	20 mm + 1 ppm	rms
	R8 GPS[7]	10 mm + 1 ppm	20 mm + 1 ppm	rms

[1] Measurement precision and accuracy in position and accuracy in height are dependent upon various factors including number of satellites, geometry, observation time, ephemeris accuracy, ionospheric conditions, multipath etc. Figures quoted assume normal to favourable conditions. Times can also not be quoted exactly. Times required are dependent upon various factors including number of satellites, geometry, ionospheric conditions, multipath etc. The following accuracies, given as root mean square, are based on measurements processed using LGO and on real-time measurements (Leica 2005).

[2] Performance dependent on location, satellite geometry, atmospheric conditions, GPS corrections, and baseline length < 10 km (NavCom 2004).

[3] Accuracy depends on the number of satellites used, obstructions, satellite geometry (DOP), occupation time, multipath effects, atmospheric conditions, baseline length, survey procedures and data quality (Sokkia 2005A, 2005B, 2006).

[4] Performance values assume minimum of 5 satellites, following the procedures recommended in the product manual. High-multipath areas, high PDOP values and periods of severe atmospheric conditions may degrade performance (Thales 2006).

[5] Specifications assume operation follows all the procedures recommended in the product manual utilizing Instant-RTK, post processing with Ashtech Solutions or Ashtech Office Suite for Survey. High-multipath areas, high PDOP values, low satellite visibility, and periods of adverse atmospheric conditions and/or other adverse circumstances will degrade system performance. All accuracy specifications are RMS values (Thales 2004).

[6] Specifications are subject to change without notice. Performance specifications assume a minimum of 6 GPS or 7 GPS/GLONASS satellites above 15 degrees in elevation and adherence to procedures recommended by TPS in the appropriate manuals. In areas of high multipath, during periods of high PDOP and during periods of high Ionospheric activity performance may be degraded. Robust checking procedures are highly recommended in areas of extreme multipath or under dense foliage (Topcon 2004, 2005).

[7] Accuracy and reliability may be subject to anomalies such as multipath, obstructions, satellite geometry, and atmospheric conditions. Always follow recommended survey practices (Trimble 2004A, 2004B, 2005).

[8] The tabulated value (10 mm + 2 ppm) is published on the manufacturer's datasheet (Thales 2004). Abousalem et al. (2001) list an accuracy specification of 10 mm + 1 ppm horizontal (standard error).

[9] Tabulated values are published by Topcon Positioning Systems (2004, 2005). Topcon Japan (2006) gives HiPer accuracy specifications 10 mm + 1.5 ppm (mse) horizontal and 15 mm + 2.0 ppm (mse) vertical. The same technology is employed in the Javad GGD-112T with accuracy specifications 10 mm + 1.5 ppm horizontal and 15 mm + 1.5 ppm vertical (Javad 2006).

[10] One-dimensional, one-sigma standard error with probability 68.3%.

[11] Accuracy level not specified on manufacturer's datasheet.

Network RTK

The accuracy values in Table 2 assume single-base RTK operation. Base station networks using the virtual reference station (VRS) concept (Landau et al. 2002; Large et al. 2001) attempt to eliminate or reduce the baseline dependent (ppm) component of the positioning errors. Accuracy figures reported by users of RTK/VRS networks vary widely, but perhaps the most thorough investigation was conducted by Häkli (2004) who reports 95% accuracies of 4.3 cm 2D horizontal and 6.7 cm 1D vertical for 2152 observations of 33 points with baseline lengths up to 78 km.

APPENDIX II. MULTIVARIATE NORMAL DISTRIBUTION

The multivariate normal distribution (Altham 2006; NIST 2006; Rice 1995) has probability density function (pdf)

$$f(\mathbf{x};\boldsymbol{\mu},\mathbf{V}) = \frac{\exp\left[-\frac{1}{2}(\mathbf{x}-\boldsymbol{\mu})^T\mathbf{V}^{-1}(\mathbf{x}-\boldsymbol{\mu})\right]}{\sqrt{(2\pi)^n|\mathbf{V}|}} \tag{6}$$

where

n = number of dimensions = degrees of freedom,
$\mathbf{x} = (x_1, x_2, \ldots, x_n)$ = column vector of random variables,
$\boldsymbol{\mu} = (\mu_1, \mu_2, \ldots, \mu_n)$ = column vector of corresponding means,
$(\mathbf{x}-\boldsymbol{\mu})^T$ = transpose of $(\mathbf{x}-\boldsymbol{\mu})$,

$$\mathbf{V} = \begin{bmatrix} \sigma_1^2 & \sigma_{12} & \cdots & \sigma_{1n} \\ \sigma_{21} & \sigma_2^2 & \cdots & \sigma_{2n} \\ \vdots & \vdots & \ddots & \vdots \\ \sigma_{n1} & \sigma_{n2} & \cdots & \sigma_n^2 \end{bmatrix} = \text{ covariance matrix,}$$

$\mathbf{V}^{-1} =$ inverse of $\mathbf{V}$, and
$|\mathbf{V}| =$ determinant of $\mathbf{V}$.

The pdf has isodensity contours

$$f(\mathbf{x};\boldsymbol{\mu},\mathbf{V}) = \text{constant} \Rightarrow (\mathbf{x}-\boldsymbol{\mu})^T\mathbf{V}^{-1}(\mathbf{x}-\boldsymbol{\mu}) = \text{constant.}$$

The boundary of the confidence region with probability p is given by the isodensity contour

$$(\mathbf{x}-\boldsymbol{\mu})^T\mathbf{V}^{-1}(\mathbf{x}-\boldsymbol{\mu}) = \chi_P^2 \tag{7}$$

where χ_P^2 is the value from the chi-square distribution (Appendix III) with n degrees of freedom that corresponds to p. When $\chi_P^2 = 1$, the region is called the one-sigma standard error region.

In the following, consider uncorrelated variables with zero mean. Then $(\mathbf{x}-\boldsymbol{\mu}) = \mathbf{x}$, and

$$\mathbf{V}^{-1} = \begin{bmatrix} \sigma_1^{-2} & 0 & \cdots & 0 \\ 0 & \sigma_2^{-2} & \cdots & 0 \\ \vdots & \vdots & \ddots & \vdots \\ 0 & 0 & \cdots & \sigma_n^{-2} \end{bmatrix}.$$

Univariate Normal Distribution

For n = 1, let $x_1 = x$ and $\sigma_1 = \sigma$. Then

$$(\mathbf{x}-\boldsymbol{\mu})^T \mathbf{V}^{-1}(\mathbf{x}-\boldsymbol{\mu}) = x\ \sigma^{-2}\ x = \frac{x^2}{\sigma^2},$$

and

$$\frac{x^2}{\sigma^2} = \chi_P^2 \Rightarrow x^2 = \sigma^2\chi_P^2 \Rightarrow x = \pm\sigma\sqrt{\chi_P^2} \qquad (8)$$

is the boundary of the confidence interval with probability p. The interval has semi-length $\sigma\sqrt{\chi_P^2}$. When $\chi_P^2 = 1$, the interval is the one-sigma standard error interval (Fig. 3) with probability 68.3%. When $\chi_P^2 = 3.8415 = 1.9600^2$ (Table 3) the interval is the 95% confidence interval (Fig. 3).

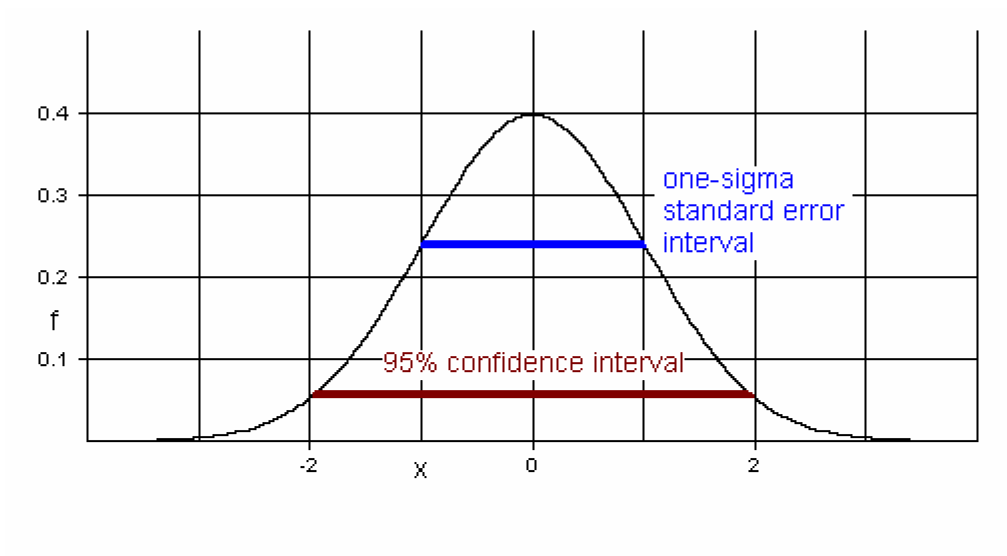

Figure 3. Confidence Intervals

Bivariate Normal Distribution

For n = 2, let $x_1 = x$, $x_2 = y$, $\sigma_1 = \sigma_x$, and $\sigma_2 = \sigma_y$. Then

$$(\mathbf{x}-\boldsymbol{\mu})^T \mathbf{V}^{-1}(\mathbf{x}-\boldsymbol{\mu}) = \begin{bmatrix} x & y \end{bmatrix} \begin{bmatrix} \sigma_x^{-2} & 0 \\ 0 & \sigma_y^{-2} \end{bmatrix} \begin{bmatrix} x \\ y \end{bmatrix} = \frac{x^2}{\sigma_x^2} + \frac{y^2}{\sigma_y^2},$$

and

$$\frac{x^2}{\sigma_x^2} + \frac{y^2}{\sigma_y^2} = \chi_P^2 \Rightarrow \frac{x^2}{\sigma_x^2 \chi_P^2} + \frac{y^2}{\sigma_y^2 \chi_P^2} = 1 \qquad (9)$$

is the boundary of the elliptical confidence region with probability p. The ellipse has semi-axes $\sigma_x\sqrt{\chi_P^2}$ and $\sigma_y\sqrt{\chi_P^2}$. When χ_P^2 = 1, the region is the interior of the one-sigma standard error ellipse (Fig. 4) with probability 39.3%. When χ_P^2 = 5.9915 = 2.4477^2 (Table 3) the ellipse is the 95% confidence ellipse (Fig. 4).

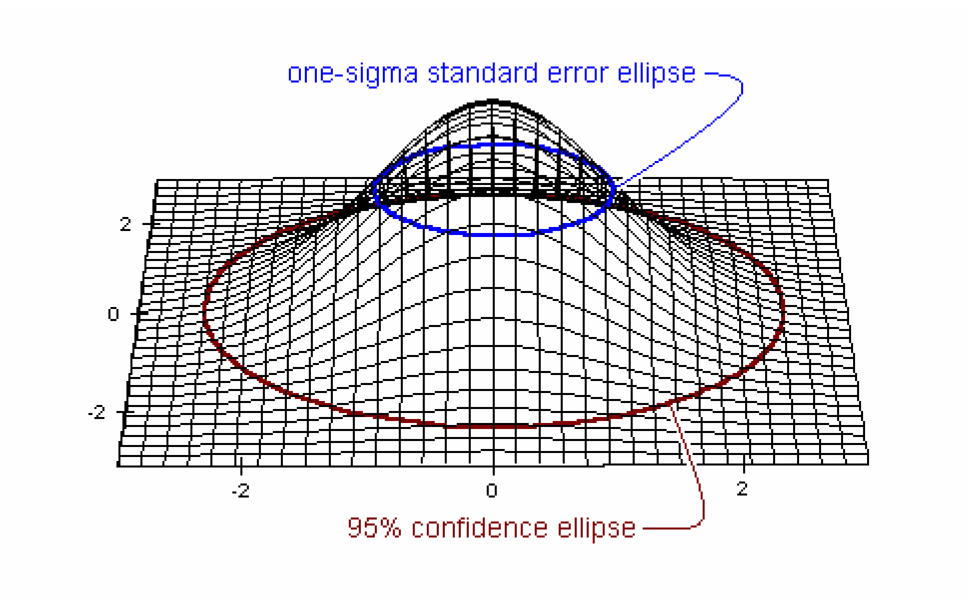

Figure 4. Confidence Ellipses

Trivariate Normal Distribution

For n = 3, let $x_1 = x$, $x_2 = y$, $x_3 = z$, $\sigma_1 = \sigma_x$, $\sigma_2 = \sigma_y$, and $\sigma_3 = \sigma_z$. Then

$$(\mathbf{x}-\boldsymbol{\mu})^T \mathbf{V}^{-1}(\mathbf{x}-\boldsymbol{\mu}) = [x \quad y \quad z]\begin{bmatrix}\sigma_x^{-2} & 0 & 0 \\ 0 & \sigma_y^{-2} & 0 \\ 0 & 0 & \sigma_z^{-2}\end{bmatrix}\begin{bmatrix}x \\ y \\ z\end{bmatrix} = \frac{x^2}{\sigma_x^2}+\frac{y^2}{\sigma_y^2}+\frac{z^2}{\sigma_z^2},$$

and

$$\frac{x^2}{\sigma_x^2}+\frac{y^2}{\sigma_y^2}+\frac{z^2}{\sigma_z^2} = \chi_P^2 \Rightarrow \frac{x^2}{\sigma_x^2\chi_P^2}+\frac{y^2}{\sigma_y^2\chi_P^2}+\frac{z^2}{\sigma_z^2\chi_P^2} = 1 \qquad (10)$$

is the boundary of the ellipsoidal confidence region with probability p. The ellipsoid has semi-axes $\sigma_x\sqrt{\chi_P^2}$, $\sigma_y\sqrt{\chi_P^2}$, and $\sigma_z\sqrt{\chi_P^2}$. When $\chi_P^2 = 1$, the region is the interior of the one-sigma standard error ellipsoid (Fig. 5) with probability 19.9%. When $\chi_P^2 = 7.8147 = 2.7955^2$ (Table 3) the ellipsoid is the 95% confidence ellipsoid (Fig. 5).

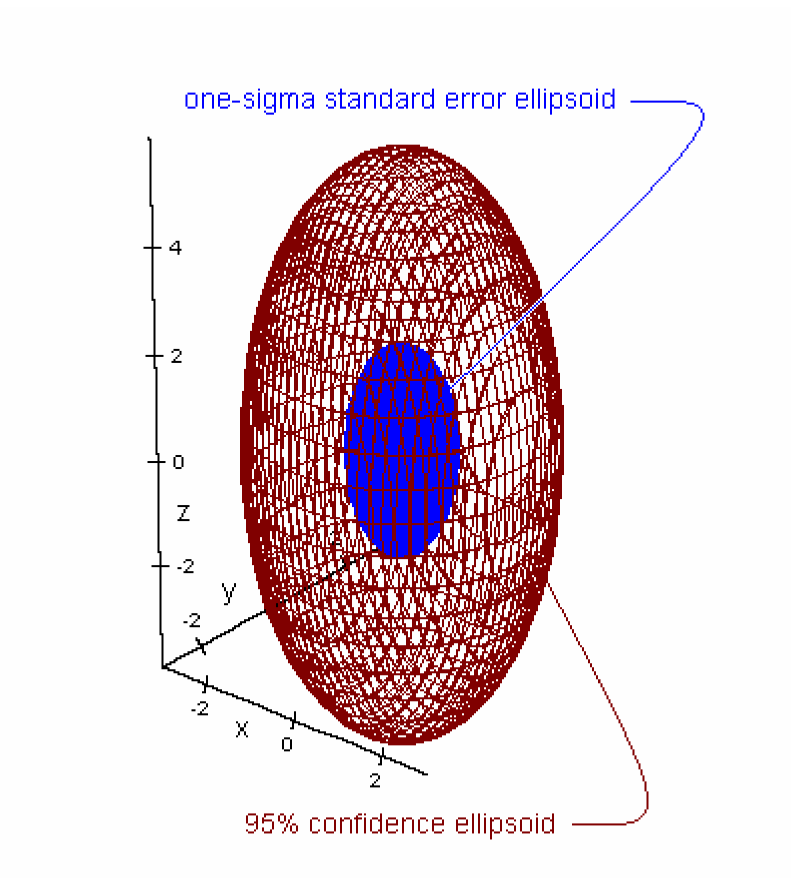

Figure 5. Confidence Ellipsoids

APPENDIX III. CHI-SQUARE DISTRIBUTION

The chi-square distribution (Rice 1995) has pdf (Fig. 6)

$$f(x;n) = \frac{x^{(n/2)-1} e^{-x/2}}{2^{n/2}\Gamma(n/2)} \tag{11}$$

where

n = degrees of freedom = number of dimensions,
x = random variable, and
Γ = gamma function.

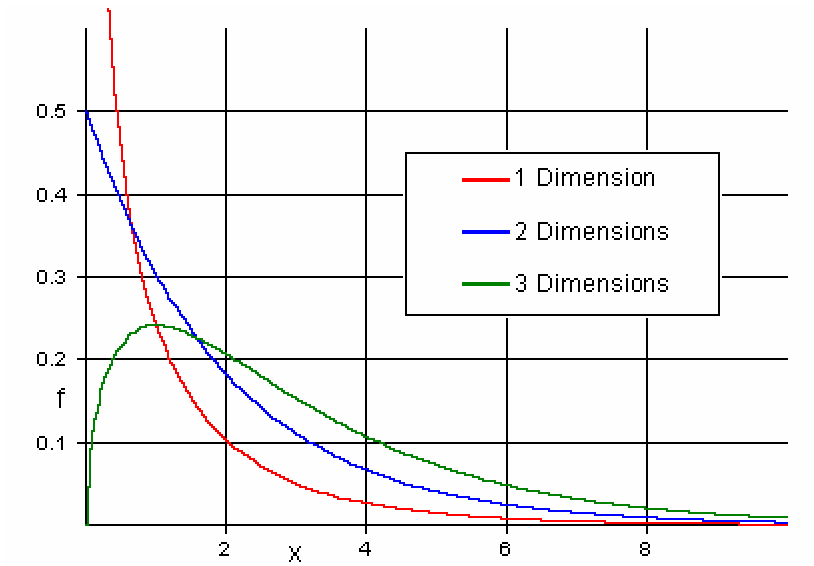

Figure 6. Chi-Square Probability Density Function

The integral of the pdf is the cumulative distribution function (cdf) (Fig. 7)

$$p(x;n) = \frac{\int_0^x \nu^{(n/2)-1} e^{-\nu/2}\, d\nu}{2^{n/2}\Gamma(n/2)}. \tag{12}$$

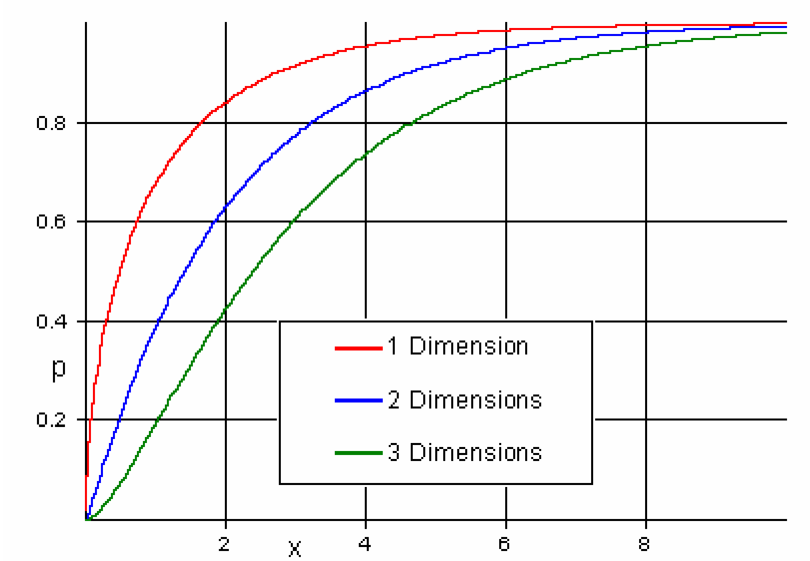

Figure 7. Chi-Square Cumulative Distribution Function

The value of x from the cdf with n degrees of freedom that corresponds to probability p is denoted by χ^2_P. The square root of χ^2_P is a factor that scales the one-sigma standard error region to the level of probability p (Fig. 8).

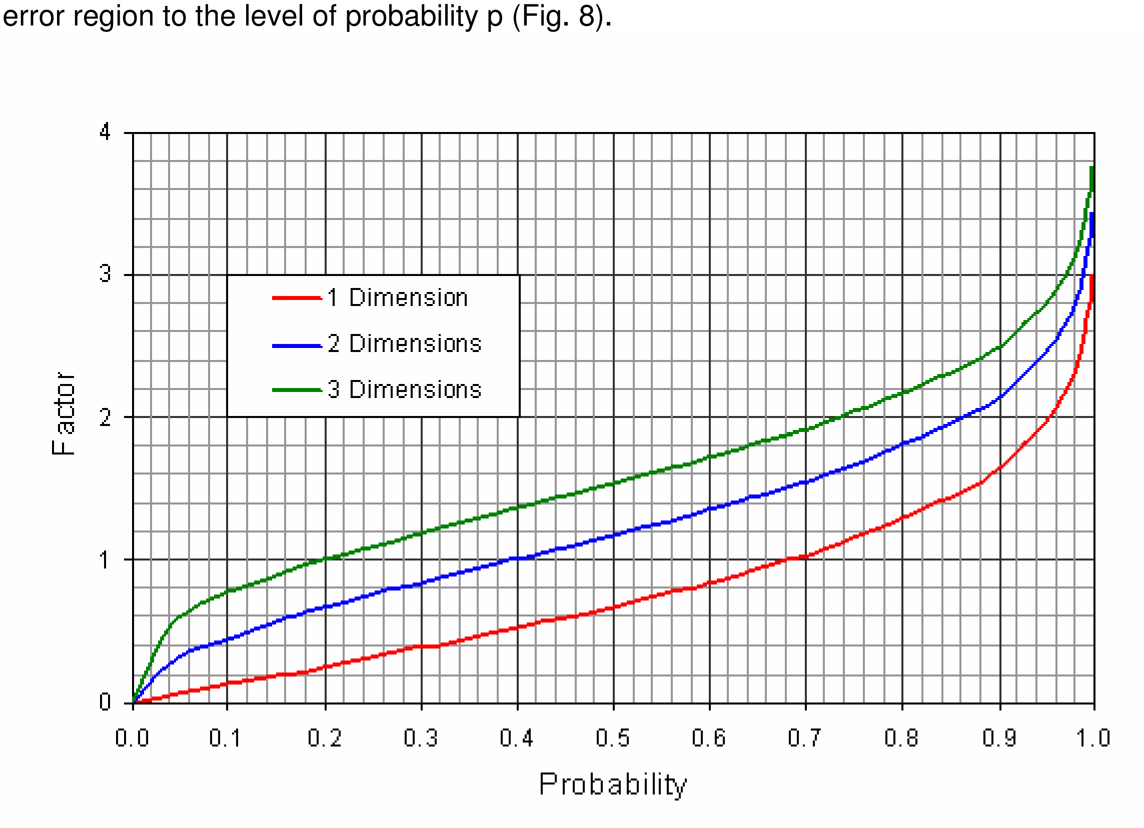

Figure 8. Confidence Region Factors

The factors in Table 3 were computed with a Microsoft Excel spreadsheet (Davis 2006) using the inverse chi-square function and show excellent agreement with values published elsewhere (FGDC 1998; James 2004; Kavanaugh 2003; NovAtel 2003; WDNR 1998) with one notable exception: Anderson and Mikhail (1998) and USACE (2003) give the 95% factor for 3 dimensions as 2.70, FGCC (1989) and ICSM (2004) give the factor as 2.79, and Alberta (2000) gives the factor as 2.795. To five significant digits, the correct value for the 3D 95% confidence region factor is 2.7955 as reported by Greenwalt and Schultz (1968).

Table 3. Confidence Region Factors

Probability	Dimensions		
	1	2	3
0.1987	0.2517	0.6657	1.0000
0.3935	0.5150	1.0000	1.3560
0.5000	0.6745	1.1774	1.5382
0.6084	0.8567	1.3693	$\sqrt{3}$
0.6321	0.9005	$\sqrt{2}$	1.7771
0.6827	1.0000	1.5152	1.8780
0.7385	1.1229	1.6380	2.0000
0.8647	1.4934	2.0000	2.3571
0.9000	1.6449	2.1460	2.5003
0.9500	1.9600	2.4477	2.7955
0.9545	2.0000	2.4860	2.8328
0.9707	2.1795	2.6572	3.0000
0.9750	2.2414	2.7162	3.0575
0.9889	2.5393	3.0000	3.3342
0.9900	2.5758	3.0349	3.3682
0.9950	2.8070	3.2552	3.5830
0.9973	3.0000	3.4394	3.7625

APPENDIX IV. CONFIDENCE REGION RADIUS

Univariate Normal Distribution

For a normally distributed variable with zero mean, the probability that an observation will be contained in the interval [-R,R] is

$$p = \frac{2}{\sigma\sqrt{2\pi}} \int_0^R \exp\left(-\frac{1}{2}\frac{x^2}{\sigma^2}\right) dx \,. \qquad (13)$$

Evaluating (13)

$$p = \operatorname{erf}\left(\frac{1}{\sqrt{2}}\frac{R}{\sigma}\right) \Rightarrow R = \sqrt{2}\,\sigma\,\operatorname{erf}^{-1}(p) \qquad (14)$$

where erf is the error function.

Bivariate Normal Distribution

For uncorrelated, normally distributed variables with zero mean, the probability that an observation will be contained in area A is

$$p = \frac{1}{\sigma_x \sigma_y 2\pi} \iint_A \exp\left[-\frac{1}{2}\left(\frac{x^2}{\sigma_x^2} + \frac{y^2}{\sigma_y^2}\right)\right] dA \,. \qquad (15)$$

Casting (15) in polar coordinates and integrating over the disk centered at the origin with radius R

$$p = \frac{4}{\sigma_x \sigma_y 2\pi} \int_0^R \int_0^{\frac{\pi}{2}} r \exp\left[-\frac{r^2}{2}\left(\frac{\cos^2\theta}{\sigma_x^2} + \frac{\sin^2\theta}{\sigma_y^2}\right)\right] d\theta \, dr \,. \qquad (16)$$

Substituting $\sin^2\theta = 1 - \cos^2\theta$

$$p = \frac{2}{\sigma_x \sigma_y \pi} \int_0^R r \exp\left(-\frac{1}{2}\frac{r^2}{\sigma_y^2}\right) \int_0^{\frac{\pi}{2}} \exp(-2\,a\,r^2 \cos^2\theta)\, d\theta \, dr \qquad (17)$$

where $a = (1/\sigma_x^2 - 1/\sigma_y^2)/4$.

Evaluating the inner integral of (17)

$$p = \frac{1}{\sigma_x \sigma_y} \int_0^R r \exp(b\,r^2)\; I_0(a\,r^2)\, dr \qquad (18)$$

where $b = -(1/\sigma_x^2 + 1/\sigma_y^2)/4$, and I_0 is the zero order modified Bessel function of the first kind.

Substituting $I_0(a\,r^2) = \sum_{k=0}^{\infty} \frac{1}{(k!)^2} \left(\frac{a\,r^2}{2} \right)^{2k}$ (Abramowitz and Stegun 1972)

$$p = \frac{1}{\sigma_x \sigma_y} \sum_{k=0}^{\infty} \frac{1}{(k!)^2} \left(\frac{a}{2} \right)^{2k} \int_0^R r^{4k+1} \exp(b\,r^2)\,dr\,. \tag{19}$$

Integrating (19) term-by-term

$$p = \frac{1}{a\,\sigma_x \sigma_y} \sum_{k=0}^{\infty} \frac{(2k)!}{(k!)^2} \left(-\frac{1}{2}\frac{a}{b} \right)^{2k+1} P(2k+1, -bR^2) \tag{20}$$

where the central binomial coefficients (Sloane 2006) $f(k) = (2k)!/(k!)^2$ are computed via the recurrence relation $f(k+1) = f(k)(4k+2)/(k+1)$, and P is the incomplete gamma function (Abramowitz and Stegun 1972).

When $\sigma_x = \sigma_y = \sigma$

$$p = 1 - \exp\left(-\frac{1}{2}\frac{R^2}{\sigma^2} \right) \Rightarrow R = \sigma\sqrt{-2\ln(1-p)}\,. \tag{21}$$

Trivariate Normal Distribution

For uncorrelated, normally distributed variables with zero mean, the probability that an observation will be contained in volume V is

$$p = \frac{1}{\sigma_x \sigma_y \sigma_z (2\pi)^{3/2}} \iiint_V \exp\left[-\frac{1}{2}\left(\frac{x^2}{\sigma_x^2} + \frac{y^2}{\sigma_y^2} + \frac{z^2}{\sigma_z^2} \right) \right] dV\,. \tag{22}$$

Casting (22) in cylindrical coordinates and integrating over the ball centered at the origin with radius R

$$p = \frac{8 \int_0^R \int_0^{\frac{\pi}{2}} r \exp\left[-\frac{r^2}{2}\left(\frac{\cos^2\theta}{\sigma_x^2} + \frac{\sin^2\theta}{\sigma_y^2} \right) \right] \int_0^{\sqrt{R^2 - r^2}} \exp\left(-\frac{1}{2}\frac{z^2}{\sigma_z^2} \right) dz\,d\theta\,dr}{\sigma_x \sigma_y \sigma_z (2\pi)^{3/2}}\,. \tag{23}$$

Evaluating the innermost integral of (23)

$$p = \frac{2}{\sigma_x \sigma_y \pi} \int_0^R \int_0^{\frac{\pi}{2}} r \exp\left[-\frac{r^2}{2} \left(\frac{\cos^2\theta}{\sigma_x^2} + \frac{\sin^2\theta}{\sigma_y^2} \right) \right] \operatorname{erf}\left(\frac{\sqrt{R^2 - r^2}}{\sqrt{2}\,\sigma_z} \right) d\theta\, dr\,. \tag{24}$$

Substituting $\sin^2\theta = 1 - \cos^2\theta$

$$p = \frac{2}{\sigma_x \sigma_y \pi} \int_0^R r \operatorname{erf}\left(\frac{\sqrt{R^2 - r^2}}{\sqrt{2}\,\sigma_z} \right) \exp\left(-\frac{1}{2} \frac{r^2}{\sigma_y^2} \right) \int_0^{\frac{\pi}{2}} \exp(-2\,a\,r^2 \cos^2\theta)\, d\theta\, dr \tag{25}$$

where $a = (1/\sigma_x^2 - 1/\sigma_y^2)/4$.

Evaluating the inner integral of (25)

$$p = \frac{1}{\sigma_x \sigma_y} \int_0^R r \operatorname{erf}\left(\frac{\sqrt{R^2 - r^2}}{\sqrt{2}\,\sigma_z} \right) \exp(b\,r^2)\;\; I_0(a\,r^2)\, dr \tag{26}$$

where $b = -(1/\sigma_x^2 + 1/\sigma_y^2)/4$.

When $\sigma_x = \sigma_y = \sigma_h$

$$p = \operatorname{erf}\left(\frac{1}{\sqrt{2}} \frac{R}{\sigma_z} \right) - \frac{1}{c} \exp\left(-\frac{1}{2} \frac{R^2}{\sigma_h^2} \right) \operatorname{erf}\left(\frac{c}{\sqrt{2}} \frac{R}{\sigma_z} \right) \tag{27}$$

where $c = \sqrt{1 - \sigma_z^2/\sigma_h^2}$ is either real or pure imaginary.

When $\sigma_x = \sigma_y = \sigma_z = \sigma$

$$p = \operatorname{erf}\left(\frac{1}{\sqrt{2}} \frac{R}{\sigma} \right) - \sqrt{\frac{2}{\pi}} \frac{R}{\sigma} \exp\left(-\frac{1}{2} \frac{R^2}{\sigma^2} \right). \tag{28}$$

Applying Newton's method to (28), R may be determined using the iteration

$$R_{k+1} = R_k + \frac{\sigma^2}{R_k} + \sqrt{\frac{\pi}{2}} \frac{\sigma^3}{R_k^2} \exp\left(\frac{1}{2} \frac{R_k^2}{\sigma^2} \right) \left[p - \operatorname{erf}\left(\frac{1}{\sqrt{2}} \frac{R_k}{\sigma} \right) \right] \tag{29}$$

with an initial estimate given by (21).

Davis and Kleder (2006) solve (18), (20), (26), (27), and (28) for radius R corresponding to probability p. Equation (5) is the result of quadratic regression on 21 radii at the 95% level for a typical RTK GPS receiver with baseline lengths from 0 to 20 km.

APPENDIX V. REFERENCES

Abramowitz, M. and Stegun, I. A., eds. (1972). *Handbook of mathematical functions with formulas, graphs, and mathematical tables*. National Bureau of Standards. 6.5.1, 7.1.23, 7.1.29, 9.6.12. (http://www.math.sfu.ca/~cbm/aands/frameindex.htm)

Abousalem, M., Han, S., Qin, X., Martin, W., and Lemoine, R. (2001). "Ashtech instant-RTK: a revolutionary solution for surveying professionals." 3rd International Symposium on Mobile Mapping Technology, Cairo, Egypt. (http://professional.magellangps.com/assets/techpapers/19_AshtechInstant-RTK.pdf)

Alberta Sustainable Resource Development (Alberta 2000). "Standards, specifications & guidelines for establishment and maintenance of Alberta survey control using GPS." (http://www.srd.gov.ab.ca/land/dos/docs/gpsrep.pdf)

Altham, P. M. E. (2006). "Applied multivariate analysis, notes." (http://www.statslab.cam.ac.uk/~pat/AppMultNotes.pdf)

Anderson, J. M. and Mikhail, E. M. (1998). *Surveying theory and practice*. McGraw-Hill, New York, N.Y.

Davis, T. G. (2006). "Confidence region factors." (http://www.eng.usf.edu/~tdavis/surveying/factors.htm)

Davis, T. and Kleder, M. (2006). "Confidence region radius." Mathworks Central File Exchange. (http://www.mathworks.com/matlabcentral/fileexchange/loadFile.do?objectId=10526&objectType=file)

Featherstone, W. E. and Stewart, M. P. (2001). "Combined analysis of real-time kinematic GPS equipment and its users for height determination." *Journal of Surveying Engineering.*, ASCE, 127(2), 31-51. (http://www.cage.curtin.edu.au/~will/getpdffile9.pdf)

Federal Geodetic Control Committee (FGCC 1989). "Geometric geodetic accuracy standards and specifications for using GPS relative positioning techniques." (http://www.ngs.noaa.gov/FGCS/tech_pub/GeomGeod.pdf)

Federal Geographic Data Committee (FGDC 1998). "Geospatial positioning accuracy standards part 3: national standard for spatial data accuracy." (http://www.fgdc.gov/standards/projects/FGDC-standards-projects/accuracy/part3/chapter3)

Florida Administrative Code (FAC 2005). "61G17 board of professional surveyors and mappers." (http://www.myflorida.com/dbpr/pro/surv/sm_fac_61g17.pdf)

Greenwalt, C. R. and Schultz, M. E. (1968). "Principles of error theory and cartographic applications." ACIC Technical Report No. 96, Aeronautical Chart and Information Center, US Air Force, St. Louis, Mo. (http://www.fgdc.gov/standards/projects/FGDC-standards-projects/accuracy/part3/tr96)

Häkli, P. (2004). "Practical test on accuracy and usability of virtual reference station method in Finland." FIG Working Week 2004, Athens, Greece. (http://www.fig.net/pub/athens/papers/ts11/TS11_4_Hakli.pdf)

Intergovernmental Committee on Surveying and Mapping (ICSM 2004). "Standards and practices for control surveys (sp1) version 1.6." (http://www.icsm.gov.au/icsm/publications/sp1/sp1v1-6.pdf)

James, F. (2004). "The interpretation of errors." (http://seal.web.cern.ch/seal/documents/minuit/mnerror.pdf)

Javad Navigation Systems (2006). "Javad GGD-112T specifications." (http://www.javad.com/index.html?/jns/products/GGD-112T.html)

Kavanaugh, B. F. (2003). *Surveying principles and applications*. Printice Hall, Upper Saddle River, N.J.
Landau, H., Vollath, U., and Chen, X. (2002). "Virtual reference station systems." *Journal of Global Positioning Systems*, 1(2), 137-143. (http://www.gmat.unsw.edu.au/wang/jgps/v1n2/v1n2pH.pdf)
Large, P., Goddard, D., and Landau, H. (2001). "eRTK: a new generation of solutions for centimeter-accurate wide-area real-time positioning." (http://trl.trimble.com/docushare/dsweb/Get/Document-6785/5700WPertkE.pdf)
Leica Geosystems (2005). "Leica GPS1200 series technical data." (http://www.leica-geosystems.com/common/shared/downloads/inc/downloader.asp?id=2670)
National Institute of Standards and Technology (NIST 2006). "The multivariate normal distribution." (http://www.itl.nist.gov/div898/handbook/pmc/section5/pmc542.htm)
NavCom Technology (2004). "NavCom RT-3010S product sheet." (http://www.navcomtech.com/docs/rt3010s.pdf)
NovAtel (2003). "GPS position accuracy measures." (http://www.novatel.com/Documents/Bulletins/apn029.pdf)
Rice, J. A. (1995). *Mathematical statistics and data analysis*. Duxbury Press, Belmont, Cal.
Sloane, N. J. A. (2006). "The on-line encyclopedia of integer sequences." AT&T Labs Research. A000984 (http://www.research.att.com/~njas/sequences/A000984)
Sokkia (2005A). "Sokkia GSR2700 IS system datasheet." (http://www.sokkia.com/Products/Detail/attachment.axd?id=153)
Sokkia (2005B). "Sokkia Radian IS system datasheet." (http://www.sokkia.com/Products/Detail/attachment.axd?id=253)
Sokkia (2006). "Sokkia GSR2600 system datasheet." (http://www.sokkia.com/Products/Detail/attachment.axd?id=214)
Thales Navigation (2004). "Z-Xtreme surveying system datasheet." (http://professional.magellangps.com/assets/datasheets/ZXtreme_EN_l.pdf)
Thales Navigation (2006). "Z-Max surveying system datasheet." (http://professional.magellangps.com/assets/datasheets/ZMax.net_EN_L.pdf)
Topcon Japan (2006). "Topcon HiPer specifications." (http://www.topcon.co.jp/eng/survey/receiver.html#gr2000)
Topcon Positioning Systems (2004). "Topcon HiPer Plus datasheet." (http://www.topconpositioning.com/library/1666_1138375830.pdf)
Topcon Positioning Systems (2005). "Topcon HiPer XT datasheet." (http://www.topconpositioning.com/library/1668_1138375830.pdf)
Trimble Navigation (2004A). "Trimble 5800 GPS system datasheet." (http://trl.trimble.com/docushare/dsweb/Get/Document-32185/5800DSE.pdf)
Trimble Navigation (2004B). "Trimble R8 GPS system datasheet." (http://trl.trimble.com/docushare/dsweb/Get/Document-265227/022543-079A_TrimbleR8GPS_DS_1204_lr.pdf)
Trimble Navigation (2005). "Trimble 5700 GPS system datasheet." (http://trl.trimble.com/docushare/dsweb/Get/Document-163620/022543-074C_5700_DS_0605_lr.pdf)
US Army Corps of Engineers (USACE 2003). "NAVSTAR global positioning system surveying." (http://www.usace.army.mil/usace-docs/eng-manuals/em1110-1-1003/entire.pdf)
Washington Department of Natural Resources (WDNR 1998). "Surveyor's guidebook on relative accuracy." (http://www.dnr.wa.gov/htdocs/plso/relacc.pdf)